PAPER

Phase behavior, rheology, and release from liquid crystalline phases containing combinations of glycerol monooleate, glyceryl monooleyl ether, propylene glycol, and water†

Hanne Evenbratt and Anna Ström [ID] *

Liquid crystalline phases can be used as slow-release matrices, where the release can be enhanced or suppressed *via* triggered phase transitions. Detailed knowledge of relevant phase diagrams is necessary, however, to control phase transitions under specific triggers. Here we complete the phase diagram of a quaternary system composed of glycerol monooleate (GMO), glyceryl monooleyl ether (GME), propylene glycol (PG), and water (W). All samples are studied at two temperatures (room and skin temperature). The liquid crystalline phases are characterized using visual inspection, small-angle X-ray diffraction (SAXD), and rheology. Cubic, reversed hexagonal, lamellar, and sponge phases are observed depending on the sample composition. The cubic and reversed hexagonal phases show typical rheological properties associated with the respective phase, *i.e.*, a stiff gel for the cubic phase with little frequency dependence, and a weaker gel whose absolute values vary with frequency in the case of the reversed hexagonal phase. Furthermore, a triggered phase transition from cubic to reversed hexagonal is observed in specific formulations upon alteration of water and PG content and temperature variation. Release of a model drug from selected compositions shows a slow release rate, where the reversed hexagonal phase reduces the release rate more than the cubic phase does. The study reveals for the first time the complete phase diagram of the quaternary system of GMO/GME/PG/W, which can be used for slow drug delivery *via* the change from the cubic phase to the reversed hexagonal phase.

Introduction

Polar lipids are able, in excess water, to self-assemble into liquid crystals.[1] Depending on their internal structure, they are classified into cubic, hexagonal and lamellar phases. Also a sponge phase can form, though such a phase is not a true liquid crystalline phase but is best described as a swelled, melted cubic phase. The liquid crystal phases are characterized by discrete lipidic hydrophobic and aqueous hydrophilic domains.[1] Such amphiphilic systems bear interest as drug delivery vehicles, since hydrophobic, hydrophilic, and amphiphilic compounds can be dissolved or dispersed within the liquid crystalline phase.[2]

The amphiphilic polar lipids glycerol monoolein (GMO) and glyceryl monooleyl ether (GME) form liquid crystalline phases in the presence of water.[3] In several studies, the cubic phase formed by GMO and water has been shown to enhance topical delivery of active pharmaceutical ingredients – for example, oregonian delivered *via* cubic phase as compared with aqueous solution,[4]

Department of Chemistry and Chemical Engineering, Pharmaceutical Technology, Chalmers University of Technology, Gothenburg, Sweden. E-mail: anna.strom@ chalmers.se

† Electronic supplementary information (ESI) available. See DOI: 10.1039/c7ra04249c

paeonol within a cubic phase as compared with microemulsion,[5] and glucosamine hydrochloride delivered through a cubic phase as compared with an oil-in-water cream or liposomal vehicle.[6] The use of a cubic phase composed of GMO has been further shown to enhance dermal delivery of δ-aminolevulinic acid (ALA), which is of particular interest when used in combination with photodynamic therapy (PDT),[7] as it may improve the treatment of thick lesions and deep-lying tumors. A major limitation for successful PDT treatment of thick lesions and deep tumors is considered to be the poor penetration of ALA.[8]

The use of cubic phases composed of GMO has, as outlined, been shown to enhance topical delivery of several pharmaceutical ingredients.[4–7] However, such formulation also poses problems. The cubic phase based on GMO is stiff in consistency, which result in high friction when applied to the skin, as well as a sticky feeling,[9] and may impair the contact between the formulation and the skin.[10] In addition, GMO is prone to hydrolysis[3] and is time-consuming to prepare, since its equilibration time is rather long. The time required to prepare a cubic phase based on GMO is a problem when it is used together with other sensitive active ingredients such as ALA.[11]

The drawbacks described above can be circumvented by the addition of propylene glycol (PG) to GMO, which softens the

GMO-based cubic phase and enhances dermal drug delivery, since it is a known permeation enhancer.[12,13] Furthermore, the use of GME instead of GMO reduces the risk of hydrolysis and enable an instantly formed cubic phase. GME forms a cubic phase in the presence of water and an aprotic solvent such as PG[14] and has been shown *in vivo* to distribute ALA and methyl-aminolevulinate equally efficiently as GMO-based cubic phases.[10] The efficient topical delivery of liquid crystalline phases is thought to be related to the structural similarity of the liquid crystalline phases and the skin.[10,15]

Liquid crystalline phases are used not only to efficiently transport active substances through the skin, but also as slow-release matrices where the release rate is controlled by diffusion[16] and specifically by the diffusion of the drug through the water domains when it comes to water-soluble substances, as in this study. The diffusion rate through the water domains of a given phase depends on the size of the active substance, the size of the water channels,[17] and the potential interaction between the active substance and the lipid matrix, *e.g.*, electrostatic.[18] Also, the geometry of the phases, *i.e.*, cubic or hexagonal phase, greatly influences the release rate. The release rate from cubic phases is typically faster than the release rate from hexagonal phases.[16] In a hexagonal phase, the drug molecule can only move along the cylindrical channel, and in a bicontinuous cubic phase in three dimensions.[19] The substance that is to be released may also need to cross into the lipid domain, which is why the release rate also depends on the lipid–water partition coefficient of the active substance.[2] Controlled release of macromolecules is achieved in, for example, hexagonal phases, where additives contribute to controlling the release rate.[20–22] Temperature[23] or pH[20] stimuli are another route to trigger reversible changes from one phase to another and thus control or suppress the drug delivery rate on demand. Detailed knowledge of the phase diagram of the specific liquid crystalline formulation is required for such attempts to succeed.

Here, we report on the effect on the drug delivery rate of a phase transition (cubic to hexagonal) triggered by temperature change and solvent evaporation. The study attempts to close missing gaps in the phase diagrams of the three-component systems of GMO/PG/water (W)[3] and GME/PG/W[14] by outlining the phases of the quaternary GMO/GME/PG/W system, which as far as the authors are aware, has not yet been done. The complete quaternary system enables formulation of "smart" materials that are responsive to temperature and/or water uptake from, *e.g.*, the skin. The phases studied are characterized using crossed polarized light, small-angle X-ray diffraction (SAXD), and rheology. We show that a reversible phase transition can be obtained *via* (a) temperature and/or (b) change in composition leading to an altered release rate of a water-soluble model drug, and confirm phase behavior using rheological methods.

Experimental section

Chemicals and materials

Glycerol monooleate (RYLO™ MG 19 Pharma, Lot no. 2202/42) was provided by Danisco Cultor (Braband, Denmark) and glyceryl monooleyl ether from Nikko Chemicals (Tokyo, Japan). The

solvent propylene glycol was obtained from Apoteket AB (Stockholm, Sweden) and the drug substitute, methylene blue, was purchased from Fluka (St. Louis, USA). Glass vials (0.7 mL) and vial caps (NTK-kemi, Uppsala, Sweden) were applied for sample preparation. All water used was of Milli-Q grade, and the chemicals were all used as supplied.

Preparation of samples

The samples were prepared in glass vials by weighing each component in the sequence of lipid(s), solvent, and water. The total sample weighed 5 g in the case of rheological and drug release studies and 0.5 g in the phase study. Thereafter, the vials were sealed and the total weight noted. For thorough mixing, centrifugation (Sigma Labex, Helsingborg, Sweden) was performed at ~4500 rcf until the samples were homogenous. The samples were left to equilibrate overnight at room temperature (approximately 20 °C).

Characterization of phases

Ocular inspection. Ocular inspections of the samples were performed to determine the number of phases present in each vial at equilibrium, the relative amount of each phase in the vial was assessed, and the order of the phases from top to bottom was noted, as well as their rheological characteristics. Signs of birefringence were studied between crossed polarizers.

The inspection was performed at two temperatures, 20 °C and 34 °C, and atmospheric pressure. The lipids were assumed to behave as single components, which has been proven to be an accurate assumption in previous studies.[14] The analysis was guided by Gibb's phase rule that, for a ternary system at room temperature, reads:

$$f = 4 - p \qquad (1)$$

where f is the degrees of freedom and p the number of phases present at equilibrium.

Small-angle X-ray diffraction. SAXD analysis was applied to determine the space group and the lattice parameter of the samples. The equipment used was a Kratky camera (Hecus X-ray Systems, Graz, Austria), equipped with a position-sensitive, 1024-channel detector (MBRAUN, Garching, Germany). Cu K_α radiation ($\lambda = 0.1542$ nm) was obtained using an X-ray generator (PW 1830/40, Philips, Amsterdam, Netherlands) operating at 50 kV and 40 mA. The analysis was performed at room temperature (20 °C). Vacuum was applied to minimize scattering from air. The distance from the sample to the detector was 275 mm and the run-time typically 1800 seconds. The instrument was calibrated using crystalline tristearin showing a lamellar structure and a lattice parameter of 4.50 nm.

Rheology. The rheological properties of the reversed hexagonal and cubic phases were studied at 20, 34, and 40 °C using an MCR 300 rheometer (Anton-Paar, Ostfildern, Germany). Plate–plate geometry was used with a diameter of 50 mm, and the gap was set to 1 mm. The measurements of elastic modulus (G') and viscous modulus (G'') were recorded as a function of time and temperature at a frequency of 0.628 rad s^{-1} and a strain of

0.01%. Frequency sweeps of the samples were performed between frequencies of 0.01 at 62.8 rads^{-1} at a constant strain of 0.01%. Strain sweeps were performed between 0.01 and 20% at a constant frequency of 0.628 rads^{-1}. The frequency and strain sweeps were done at $T = 20\ ^\circ C$ unless otherwise stated. A solvent trap was used to minimize water loss by evaporation during the measurements, and the temperature was controlled by a Peltier system. The samples were allowed to equilibrate for 15 min after loading prior to the start of the measurement.

Drug release

Each formulation was applied in a disk with a 0.5 cm^3 recess (2.5 cm^2 area exposed to the water) and lowered into a USP bath (Dissolutest, Prolabo) with 1 L vessels belonging to the USP bath containing 250 mL. The water surrounding the vessel was set at $T = 34\ ^\circ C$. The paddle (USP Dissolutest, Prolabo) was rotating at 50 rpm and placed 2.5 cm above the disk. A 2 mL sample was removed and replaced by water at increasing intervals during one week. The absorbance was measured for each sample using a UV spectrophotometer (Cary 60 UV-Vis, Agilent Technologies, Santa Clara, USA) at the wavelength of 664 nm using a quartz cuvette. The concentrations were calculated based on a standard curve ($R^2 = 0.9979$) and the Beer–Lambert law:

$$A = \varepsilon l c \qquad (2)$$

where l is the length of the cuvette, ε the molar absorptivity (obtained from the standard curve), and c the concentration.

Results and discussion

Dual lipid-based liquid crystalline phases, formed in combination with water and solvent, were compared in order to thoroughly investigate how the formulations influence the phase behavior, rheology, and drug release. The phase study was based on previously published results describing three phase diagrams: GMO/PG/W, GME/PG/W, and GMO/GME/W.[3,14] To complete the picture, all four components were combined and studied at temperatures relevant for storage and use as skin formulations.

Topical delivery (in this case focused mainly on dermal delivery) of drugs bears high patient compliance and the possibility of achieving both local and systemic effects of the drug. In the case of systemic effect, topical drug delivery adds the advantage of simple circumvention of first-pass metabolism. However, one of the main purposes of this organ is to prevent entry of foreign substances into the body, which puts high demands on the formulations and their interaction with the skin.

Specific phases, *i.e.*, formulations, were chosen for rheology and drug release studies. The water content was chosen according to its similarities with dermal drug administration. Specifically, 20% water and 20 °C were comparable to the situation before application on the skin surface, with 43% water and 34 °C being chosen to mimic the situation the formulation meets after skin application – for example, due to trans-epidermal water loss and body heat.

Phase behavior

The four components were combined in the relative amounts shown as dots in Fig. 1. Visual inspection is a useful preliminary tool for identifying different phases according to such factors as their relative density and viscosity. Adding crossed polarizers enables distinction between phases that to the naked eye may seem identical. For example, the cubic and the reversed hexagonal phases can be distinguished, since the latter appears to be shining when observed through crossed polarizers due to birefringence. Some of the samples were chosen for SAXD analysis to determine phase characteristics for the ordered structures such as cubic and reversed hexagonal. The observations were summed up in phase diagrams showing the liquid crystalline phases that are formed at different water content and temperatures. Fig. 2 depicts (adapted) previously published phase diagrams. Together with the new observations, it is now possible to paint a more complete picture of the phase behavior of this system at both different temperatures and differing water content.

When excluding water, while combining GMO, GME, and PG, no liquid crystalline phases were formed. Solid lipid could be found at concentrations of the solvent (PG) below 40% at 20 °C. At 34 °C, all samples were liquids through and through.

By focusing on the four-component system with different amounts of water at varied temperatures, the complete tetrahedron can be visualized.

The four components were, as previously mentioned, GMO, GME, PG, and W. Observations are presented for GMO, GME, and PG with (a) 20% W at 20 °C and 34 °C, as well as with (b) 43% W at 20 °C and 34 °C.

(a) At 20 °C and 10% PG, samples containing high amounts of GMO formed a lamellar phase. Increasing the amount of GME resulted in first the cubic phase and then the reversed hexagonal phase. Adding more PG to the samples favored the lamellar phase. The sponge phase was formed at high concentrations of PG and in the absence of GMO.

At 34 °C and 10% PG, lamellar, cubic, and reversed hexagonal phases were found. The sponge phase was formed only at high amounts of PG and GMO. Some changes in phase behavior were observed that contrasted with the situation at 20 °C: the reversed hexagonal and sponge phases were favored at the higher temperature.

(b) All samples contained two to three layers/phases as expected, since 43% water was calculated to amount to excess water. At 20 °C and 10% PG, cubic phases were formed at high GMO concentrations. Increased amounts of GME favored the reversed hexagonal phase. This was counteracted when the PG content was increased, which increased the presence of the cubic phase. All samples were cubic at 40% PG, regardless of the GMO/GME composition. At 50% PG and high concentrations of GMO, three layers were observed: cubic phase, sponge phase, and an excess of water and PG solution.

At 34 °C and 43% water, the sponge phase was observed at 50% PG and a high concentration of GMO. The cubic phase was favored as the amount of PG was increased. Some changes in phase behavior were observed when less water was included:
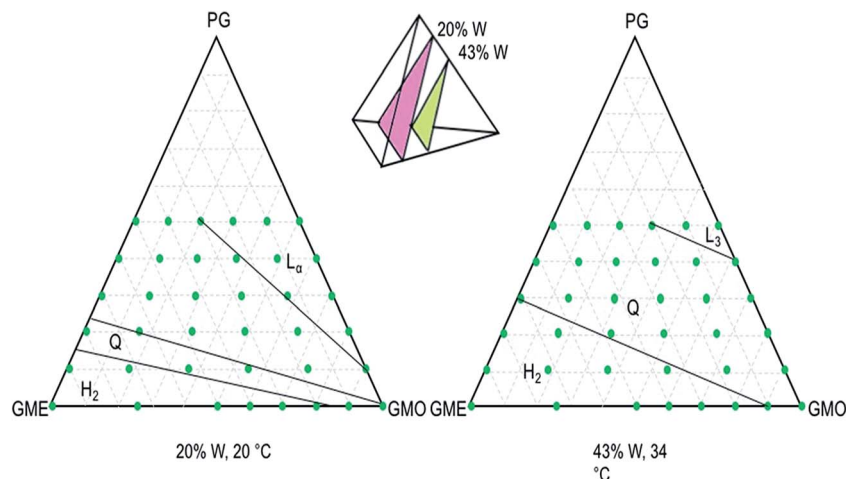
Fig. 1 The tetrahedron represents the complete GMO/GME/PG/W quaternary system. The two marked slices denote the two-phase diagrams at 20% and 43% water. The phase diagrams shown are to the left: 20% water and 20 °C, and to the right: 43% water and 34 °C. Dots mark the included samples. The letters denote as follows: H_2 reversed hexagonal phase, L_α lamellar, L_3 sponge, and Q cubic.
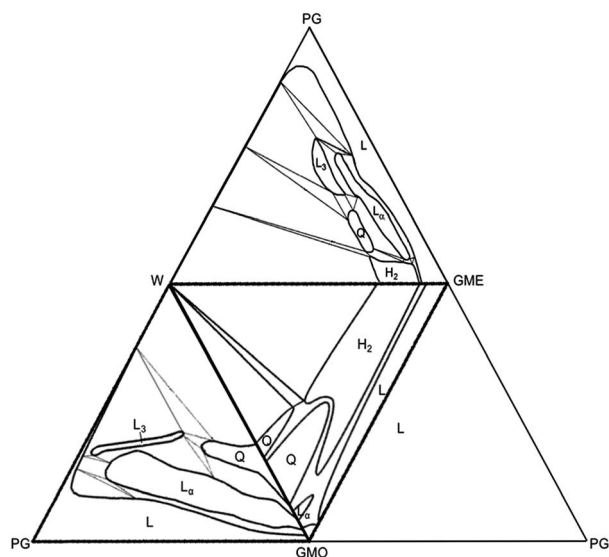

Fig. 2 Adapted unfolded tetrahedron from Popescu and co-workers as well as Engström and co-workers of phase diagrams using the components GMO, GME, PG, and W at 20 °C. The letters denote as follows: H_2 reversed hexagonal phase, L liquid, L_α lamellar, L_3 sponge, and Q cubic.[3,14]

the reversed hexagonal and sponge phases were favored. In the absence of PG, the reversed hexagonal phase was favored at the increased temperature.

All samples containing 43% water, regardless of the temperature, showed a layer of excess water (and PG) in the bottom of the vial. The height of this layer was dependent on the amount of GME and GMO in the sample. The water layer was largest in samples containing more GME. This is due to the greater ability of GMO phases to swell in water and thus contain a higher volume of water.

Different formulations, GMO/W, GME/W, GMO/GME/W, GME/PG/W, and GMO/PG/W, were selected for their

rheological characterization and ability to act as sustained-release formulations. The exact composition of the five formulations, as well as their crystalline phase at 20 °C, is presented in Table 1.

Typical SAXD patterns corresponding to the reversed hexagonal phase and the cubic phase (in maximally swollen state) are shown in ESI, Fig. 1.† The similar SAXD pattern of the cubic phase prior and post phase transition (triggered by temperature) shows that the phase transition is reversible upon temperature cycling (ESI Fig. 1†).

Drug release studies

Drug release of a hydrophilic molecule, methylene blue, was studied from selected formulations with a reversed hexagonal or cubic initial structure. These phase structures were chosen because of their slow/sustained release properties and texture that makes them suitable as dermal drug delivery formulations, and also previously published results indicating a favorable phase transition that enhances drug delivery into the skin.[10]

As mentioned, one of the main purposes of the skin is to act as a barrier. The lipids of the skin are a very important part of this function. Mainly, the lipids are in a rigid state at 32 °C with a small amount of fluid lipids present.[24,25] Lamellar and reversed hexagonal liquid crystalline phases have been found to

Table 1 Composition of samples studied using rheology and as slow-release matrices

Formulation (%)				Liquid crystalline phase at $T = 20$ °C
W	GMO	GME	PG	
20	80			Cubic
35	50		15	Cubic
24		61	15	Cubic
24	64	16		Cubic
20		80		Hexagonal

exist,[26] and by influencing the borders of the rigid parts – for instance, by hydration or diffusion of solvents – other phase changes may occur. These naturally occurring phase changes are highly relevant for this study, since phase changes and alterations in hydration would be influenced by applying the chosen formulations to the skin.

The results of this drug release study showed, as expected,[16] a faster release of a higher amount of methylene blue from the cubic phases, decreasing for the cubic phases that turned into reversed hexagonal phases in excess water, and a very small amount from the reversed hexagonal phase (Fig. 3a).

The GMO-based formulations can swell their water channels, thus holding more water than the GME-based formulations, owing to the packing structure of the respective molecules. Also, when changing from a cubic to a reversed hexagonal phase, the release will decrease, since a reversed hexagonal structure contains fewer possibilities for the drug to diffuse out of the structure. The long cylindrical channels of the reversed hexagonal phase enclose the water-soluble pharmaceutics more than the bicontinuous lipid bilayer structure with

Fig. 3 Release data from GMO/PG/W (black triangles), GMO/GME/W (black circles), GME/PG/W (unfilled circles), and GME/W (grey squares) presented as (a) function of time and (b) square root of time with linear fit (dashed line), where release was measured in excess of water and at $T = 34 \,^\circ C$.

two-water channel systems, *i.e.*, the cubic phase.[27,28] Plotting the release data of the different compositions *versus* square root of time, the data show a linear relationship indicating that diffusion is the dominant release mode (Fig. 3b), for all phases in agreement with previous studies.[16,17] The slope of the cubic phase is 1.7 ($r^2 = 0.96$) is the highest and the slope of the reversed hexagonal phase with a of 0.17 ($r^2 = 0.93$), the lowest. The composition exhibiting reversible phases show both a higher slope of 0.40 ($r^2 = 0.95$) and 0.31 ($r^2 = 0.92$) compared to the reversed hexagonal phase. Further work is in progress where the initial part of the release curves are studied in more detail and with specific focus on determining whether the initial release from the cubic phase can be identified followed by the lower hexagonal phase *e.g. via* fitting of two different lines, one corresponding to the faster release from cubic phase and the other from the slower release typical of the reversed hexagonal phase.

The start and end phases of the selected formulations used for the drug release studies are shown in Table 2. SAXD analysis was performed on the samples before and after the release studies in a USP bath. All formulations that contained GME ended as reversed hexagonal after being subjected to excess 34 °C water, regardless of the starting phase. These phase transitions depend mainly on the release of PG into the surrounding water, and the temperature. The release of PG and the elevated temperature affect the formulations to a varying extent. The formulation containing GME/PG/W will go from cubic to reversed hexagonal at a PG decrease of less than 5%.[14] An elevated temperature will push the cubic phase toward the reversed hexagonal in the GMO/GME/W system.[3] In the phase diagrams shown in Fig. 1, the same trend is evident. A decrease in PG and an increase in temperature favor the reversed hexagonal phase before the cubic phase.

Completion of the quaternary system enables prediction of phase transitions at conditions (*e.g.* temperature, humidity/wetness) relevant to cosmetic or pharmaceutical applications (see Fig. 3). Fig. 2 and Table 2 can be used to further explain Fig. 3. The phase transitions that occur during the release experiments are restricted to the possibilities shown in the phase diagrams. GMO/PG/W started as cubic, PG increases the water channel diameter (increase swelling of the structure), but is also slowly released into the surrounding water. However, release of PG does not induce a phase transition as the GMO/W system is a stable cubic phase under these conditions. GMO/GME/W starts as cubic in the proportions chosen but is
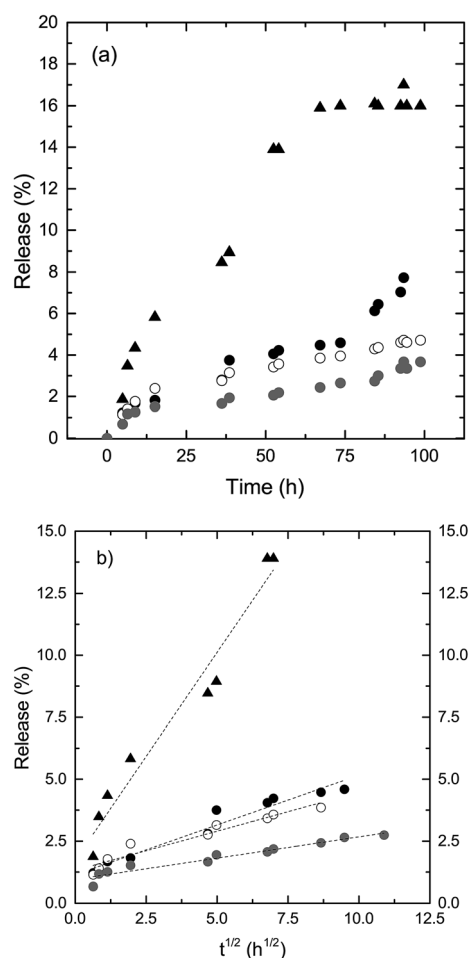
Table 2 Composition of the liquid crystalline phases, with different starting geometries that in some cases altered when in excess water and higher temperature during the release and rheological studies

Formulation	Start phase	End phase
W/GMO	Cubic	Cubic
W/GMO/PG	Cubic	Cubic
W/GMO/GME	Cubic	Hexagonal
W/GME/PG	Cubic	Hexagonal
W/GME	Hexagonal	Hexagonal

sensitive to temperature.[3] Increasing temperature favours the reversed hexagonal phase. GME/PG/W started as cubic with maximally waterfilled channels. With time PG is released along with the model drug, though the GME/W ratio remains constant. Release of PG induces a phase transition from cubic to reversed hexagonal, as seen in Fig. 2. GME/W will, under these conditions, remain a reversed hexagonal and, as has been mentioned, have the least favorable structure for drug release. As can be noted from Fig. 3, the amount released after one week is low for all compositions tested. This finding indicates that these systems provide extended release and thus could be used to reduce dosing frequency.[16,18] As has been previously shown, the drug release into the skin from some of these systems enables deep penetration from a formulation depot in the upper layers of the skin.[7,10] However, direct release is not necessarily sought when it comes to dermal drug delivery. Thus, a very slow release can be positive in this case as it takes time for the skin and the formulation to interact. A depot effect or droplet release from the applied formulation that best cooperates with the skin composition and structure would prove the most efficient delivery strategy.[15]

Rheological characterization

The viscoelastic characteristics of the different compositions were determined using rheological measurements. The storage modulus (G') and the loss modulus (G'') were measured as a function of frequency and time. G' and G'' reflect the elastic (solid) and the viscous (liquid) properties, respectively. Tan δ values were derived from the values of G' and G'' according to tan $\delta = G''/G'$. Thus, a purely elastic sample gives tan δ approaching 0 and a purely viscous sample gives values of 1 or above.

GMO/W, GMO/GME/W, GME/PG/W, and GMO/PG/W were characterized as cubic phases at 20 °C. The general behavior of G' and G'' as a function of frequency is similar for all cubic phases studied and is in line with previous studies on cubic phases composed of Dimodan and water,[29] and using GMO/diglycerol monooleate/W.[30]

The general behavior of G' and G'' as a function of frequency is illustrated by the sample containing GMO/PG/W (GMO/W is shown in ESI Fig. 2†). As shown in Fig. 4a, G'' predominates at lower frequencies, while G' is dominant at higher frequencies. The frequency at which the crossover, $G' > G''$, occurs depends on the composition of the sample. While the value of G' levels out after an initial increase, G'' is continuously reduced with increasing frequencies. The change from a predominantly liquid-like behavior to solid with increasing frequency is further reflected by tan δ going from values close to 1 at low frequency, followed by a rapid decrease at the G'/G'' crossover, and finally leveling out at tan δ values close to 0.

The relaxation time of the systems is obtained from the frequency at which $G' > G''$ and describes the time required for the water–lipid interface to relax to or obtain equilibrium configuration, after having been perturbed by shear deformations.[29] The maximum relaxation time (τ_{max}) is given by $\tau_{max} \sim 1/\omega$, where ω is the frequency at the crossover of $G' > G''$. The
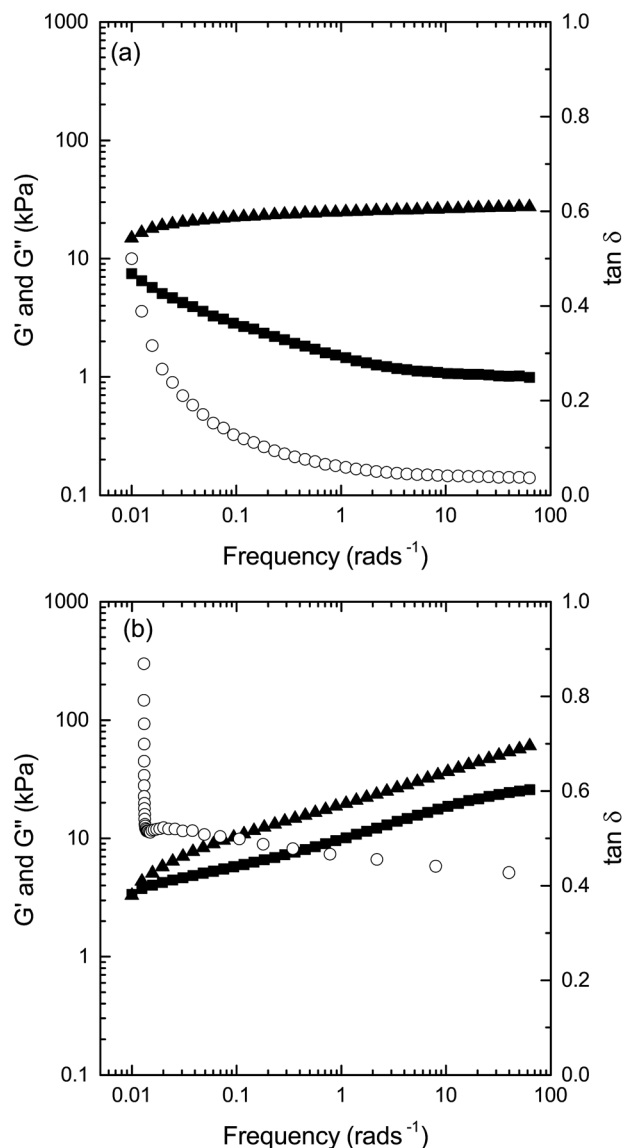

Fig. 4 G' (triangles), G'' (squares), and tan δ (open circles) as a function of frequency of cubic phase composed of (a) 50 : 15 : 35 (wt%) GMO/PG/W, and (b) reversed hexagonal phase composed of 80 : 20 (wt%) GME and W, at a strain of 0.01% and $T = 20$ °C.

relaxation time of the samples studied is reduced in the series of GMO/W ($\tau_{max} \sim 100$ s) > GMO/GME/W ($\tau_{max} \sim 50$ s) > GME/PG/W ($\tau_{max} \sim 33$ s), thus confirming that the cubic phases based on GME obtain equilibrium faster than the phases based on GMO.[10] It should be noted that the relaxation times of GMO/PG/W were long, as the G'/G'' crossover occurs at lower frequencies than the frequencies used in this study.

Comparing the strength of the different samples, we observed reducing strength in the series of GMO/W > GMO/GME/W > GMO/PG/W $\geq$ GME/PG/W (Table 3). The series is in line with a commonly quoted notion that a GME-based cubic phase is less stiff than a GMO-based cubic phase. Furthermore, we observed a reduction in strength of the GMO-based cubic phase by the addition of GME and, as expected,[12] by the use of PG as a solvent.

Table 3 G' and tan δ of the different compositions at $T = 20$, 34, and 40 °C as determined at $t = 35$ min, $f = 0.628$ rad s^{-1}, and strain = 0.01%

Sample	$T = 20$ °C		$T = 34$ °C		$T = 40$ °C	
	G'/kPa	tan δ	G'/kPa	tan δ	G'/kPa	tan δ
Cubic phases						
W/GMO	630 ± 60	0.19	480 ± 50	0.53	370 ± 36	0.71
W/GMO/PG	25 ± 3	0.06	24 ± 2	0.06	24 ± 2	0.06
W/GME/PG	50 ± 5	0.31	43 ± 4	0.33	25 ± 2	0.33
W/GMO/GME	93 ± 9	0.25	53 ± 5	0.46	—	—
Reversed hexagonal phases						
W/GME	18 ± 2	0.56	12 ± 1	0.69	10 ± 1	0.80
W/GMO/GME	—	—	—	—	6 ± 0.5	0.67

The sample characterized as reversed hexagonal phase (GME/W) shows a markedly different frequency dependence of the moduli (Fig. 4b). As for the cubic phase, G'' is larger than G' at low frequencies. However, while G'/G'' crossover occurs at higher frequencies, both G' and G'' increase with the frequency, instead of the observed reduction in G'' and leveling out of the value of G' as observed for the cubic phase. Furthermore, the difference between G' and G'' is smaller than that observed for the cubic phase, resulting in a slowly reducing, but still relatively high, tan δ (between 0.5 and 0.4) over the intermediate frequency sweep tested for the reversed hexagonal phase.

Time sweeps were performed at three temperatures (20, 34, and 40 °C), to determine how the values of the moduli varied with temperatures relevant for topical use. The results reflect the generally increased solid-like behavior of the cubic phase (larger difference between G' and G'' resulting in a lower tan δ) compared with the reversed hexagonal phase (except for temperatures > 20 °C) (Table 3). G' is considerably decreased and tan δ increased for GMO/W, indicating that this particular sample becomes considerably weaker and more liquid-like (while retaining the cubic phase) with a temperature increase to 40 °C, in agreement with previous studies.[29] In contrast, increasing the temperature from 20 to 40 °C did not influence the cubic phase composed of GMO/PG/W, since both tan δ and G' are close to constant. The sample of GME/PG/W shows a reduction in both G' and G'', resulting in a constant value of tan δ.

A phase transition from cubic to reversed hexagonal was observed for the sample composed of GME/GMO/W with a temperature increase from 20 to 40 °C. This sample shows an important reduction in G' (15×) at $T = 40$ °C compared with $T = 20$ °C, and an increase in tan δ from 0.27 to 0.7 (values of G', G'' at $T = 20$, 34 and 40 °C are presented in ESI†). In addition, the frequency behavior of the moduli of this particular sample at $T = 20$ °C and $T = 40$ °C demonstrates the typical frequency behavior of the cubic phase at $T = 20$ °C (Fig. 5a) and the reversed hexagonal phase at $T = 40$ °C (Fig. 5b). Temperature cycling 1 from 40 to 20 °C show that the phase changes are reversible (in agreement with SAXD data). Upon temperature reduction from 40 to 20 °C, the sample show again higher values of moduli, low tan δ and frequency behaviour typical of the cubic phase (results shown as ESI, Fig. 3†).
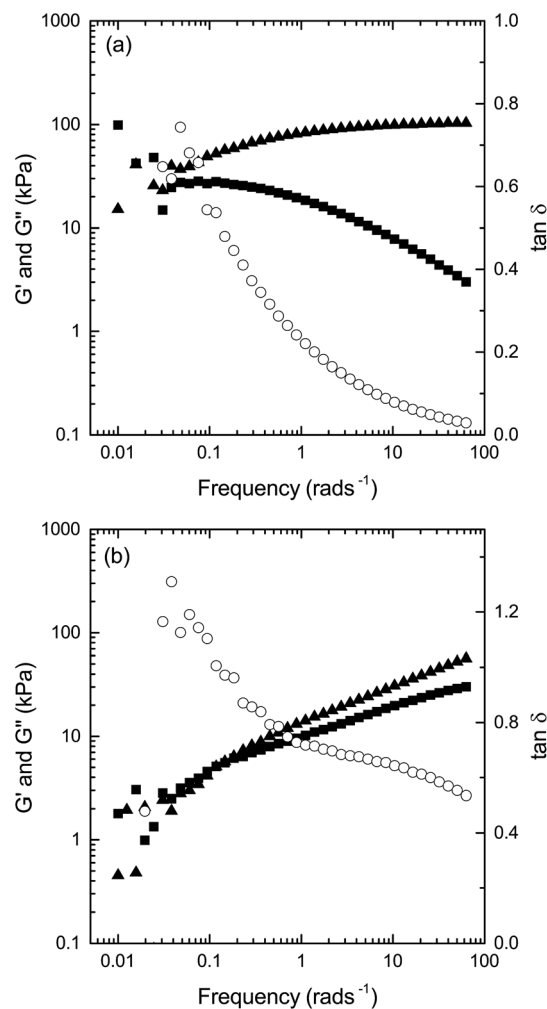

Fig. 5 G' (triangles), G'' (squares), and tan δ (open circles) as a function of frequency for 64 : 16 : 20 (wt%) GMO/GME/W composition at (a) $T = 20$ °C and (b) $T = 40$ °C and a strain of 0.01%.

Not only does the rheology of the different compositions give insight into the possibilities of practical use of the compositions, such as process ability and stiffness at application *via* topical use or injection, but also the results presented here confirm the findings of previous studies[29] showing that phase transitions between cubic and reversed hexagonal phases triggered by, for example, compositional change or temperature are rapidly detectable *via* rheological means.

Conclusions

The phase diagram of the four-components system of GMO/GME/PG/W showed high dependence on water content and temperature alteration.

At 20% water content, high amounts of GMO favored the lamellar phase. Increasing the amount of GME resulted in the cubic phase and then the reversed hexagonal phase. Increasing the PG content would favor the lamellar phase, and the sponge phase was only observed in the absence of GMO. Increasing the

temperature from 20 to 34 °C would instead favor the reversed hexagonal and sponge phases.

Increasing the water content from 20 to 43% water resulted in an additional layer or phase, since water was present in excess. In this situation, increasing amounts of GME favored the hexagonal phase. Such behavior could be balanced by increasing the amount of PG, resulting in the presence of a cubic phase. All samples were cubic at 40% PG, regardless of the GMO/GME composition.

The release rates of methylene blue from the cubic and hexagonal phases were slow and lasted for several days. The release rate was clearly more rapid for the cubic phase. Furthermore, complete release was not obtained.

Both the cubic and the reversed hexagonal phase exhibited typical rheological properties. The cubic phase was stiff and showed little frequency dependence at the frequencies tested. In comparison, the hexagonal phase was less stiff and its moduli were more dependent on the frequency. Furthermore, the rheological characterization revealed phase transitions from, for example, the cubic to the hexagonal phase upon an increase in temperature, thus showing promise as a convenient tool for following the phase changes of liquid crystalline phases during, for example, the preparation of formulations. The observed phase changes and rheological properties at a relatively small temperature range are well suited for, e.g., dermal formulations.

Acknowledgements

References

1 T. Kaasgaard and C. J. Drummond, *Phys. Chem. Chem. Phys.*, 2006, **8**, 4957–4975.
2 S. Engström, T. P. Nordén and H. Nyquist, *Eur. J. Pharm. Sci.*, 1999, **8**, 243–254.
3 G. Popescu, J. Barauskas, T. Nylander and F. Tiberg, *Langmuir*, 2007, **23**, 496–503.
4 T.-J. K. Im, M. Joo, D.-W. Seo and J.-H. Lee, *Biomol. Ther.*, 2008, **16**, 226–230.
5 M. Luo, Q. Shen and J. Chen, *Int. J. Nanomed.*, 2011, **6**, 1603–1610.
6 I. H. Han, S.-U. Choi, D. Y. Nam, Y. M. Park, M. J. Kang, K. H. Kang, Y. M. Kim, G. Bae, I. Y. Oh, J. H. Park, J. S. Ye, Y. B. Choi, D. K. Kim, J. Lee and Y. W. Choi, *Arch. Pharmacal Res.*, 2010, **33**, 293–299.
7 J. Bender, M. B. Ericson, N. Merclin, V. Iani, A. Rosén, S. Engström and J. Moan, *J. Controlled Release*, 2005, **106**, 350–360.
8 C. Sandberg, C. B. Halldin, M. B. Ericson, O. Larkö, A. L. Krogstad and A. M. Wennberg, *Br. J. Dermatol.*, 2008, **159**, 1170–1176.
9 L. Skedung, I. Buraczewska-Norin, N. Dawood, M. W. Rutland and L. Ringstad, *Skin Res. Tech.*, 2016, **22**, 46–54.
10 H. Evenbratt, C. Jonsson, J. Faergemann, S. Engström and M. B. Ericson, *Int. J. Pharm.*, 2013, **452**, 270–275.
11 M. Kaliszewski, M. Kwasny, A. Juzeniene, P. Juzenas, A. Graczyk, L.-W. Ma, V. Iani, P. Mikolajewska and J. Moan, *J. Photochem. Photobiol., B*, 2007, **87**, 67–72.
12 B. W. Barry, *J. Controlled Release*, 1987, **6**, 85–97.
13 R. B. Walker and E. W. Smith, *Adv. Drug Delivery Rev.*, 1996, **18**, 295–301.
14 S. Engström, P. Wadsten-Hindrichsen and B. Hernius, *Langmuir*, 2007, **23**, 10020–10025.
15 H. Evenbratt, L. Nordstierna, M. B. Ericson and S. Engström, *Langmuir*, 2013, **29**, 13058–13065.
16 B. J. Boyd, D. V. Whittaker, S.-M. Khoo and G. Davey, *Int. J. Pharm.*, 2006, **309**, 218–226.
17 R. Negrini and R. Mezzenga, *Langmuir*, 2012, **28**, 16455–16462.
18 J. Clogston and M. Caffrey, *J. Controlled Release*, 2005, **107**, 97–111.
19 A. Zabara and R. Mezzenga, *J. Controlled Release*, 2014, **188**, 31–43.
20 N. B. Bisset, B. J. Boyd and Y.-D. Dong, *Int. J. Pharm.*, 2015, **495**, 241–248.
21 T. Mishraki, M. F. Ottaviani, A. I. Shames, A. Aserin and N. Garti, *J. Phys. Chem. B*, 2011, **115**, 8054–8062.
22 T. Mishraki-Berkowitz, A. Aserin and N. Garti, *J. Colloid Interface Sci.*, 2017, **486**, 184–193.
23 W.-K. Fong, T. Hanley and B. J. Boyd, *J. Controlled Release*, 2009, **135**, 218–226.
24 J. Bouwstra, G. Gooris and M. Ponec, *J. Biol. Phys.*, 2002, **28**, 211–223.
25 S. Guldbrand, V. Kirejev, C. Simonsson, M. Goksör, M. Smedh and M. B. Ericson, *Eur. J. Pharm. Biopharm.*, 2013, **84**, 430–436.
26 S. Björklund, T. Ruzgas, A. Nowacka, I. Dahi, D. Topgaard, E. Sparr and J. Engblom, *Biophys. J.*, 2013, **104**, 2639–2650.
27 S. Hyde, S. Andersson, B. Ericsson and K. Larsson, *Z. Kristallogr.*, 1984, **168**, 213–219.
28 R. G. Laughlin, *The aqueous phase behavior of surfactants*, Academic Press, 1994.
29 R. Mezzenga, C. Meyer, C. Servais, A. I. Romoscanu, L. Sagalowicz and R. C. Hayward, *Langmuir*, 2005, **21**, 3322–3333.
30 P. Pitzalis, M. Monduzzi, N. Krog, H. Larsson, H. Ljusberg-Wahren and T. Nylander, *Langmuir*, 2000, **16**, 6358–6365.